Study of the Influence of Xanthate Derivative Structures on Copper Sulfide Mineral Adsorption Under Acidic Conditions

D.M. ÁVILA-MÁRQUEZ, I.A. REYES-DOMÍNGUEZ, A. BLANCO-FLORES, H.P. TOLEDO-JALDIN, G. LÓPEZ-TÉLLEZ, J. AGUILAR-CARRILLO, and E.J. GUTIÉRREZ-CASTAÑEDA

Adsorption of commercial xanthate derivatives on copper sulfide mineral (covellite, CuS) was studied by kinetics and isotherm adsorption experiments. The adsorption of xanthate derivatives was confirmed by FTIR (Fourier transform infrared spectroscopy) and XPS (X-ray photoelectron spectroscopy) results. Experiments were performed with two different xanthate derivatives, C-4410 (*O*-pentyl *S*-2-propenyl ester) and C-4940 (isobutyl xanthogen ethyl formate), on individual doses of 0.05 g of powdered covellite. It was found that the equilibrium times at pH 2, 4, and 6 were different for both xanthate derivatives. The shortest times were achieved at pH 2 and 4. The results suggest that C-4110 can be used as collector in a wide range of pH, while C-4940 is limited to lower pH values. Pseudo first- and pseudo second-order kinetics models were thus applied to the experimental data for pH 2. The information obtained from the kinetics models combined with XPS allowed proposing the adsorption mechanism for the covellite-xanthate derivative pair. The adsorption takes place through a non-covalent interaction for C-4410 and chemisorption process for C-4940. The best-fitting isotherm models for C-4410 and C-4940 adsorption were Redlich–Peterson and Freundlich, respectively, which yield a maximum adsorption capacity of 57.07 mg g^{-1} for C-4410 and 44.62 mg g^{-1} for C-4940.

https://doi.org/10.1007/s11663-018-1452-z

I. INTRODUCTION

CURRENTLY, the mining and metallurgical industries are interested not only in optimization of conventional methods of minerals concentration from natural deposits, but also in investigating new alternatives that allow to recover valuable species from other sources, such as leaching residues. Most of these wastes are generated at extremely acid conditions, which make it difficult to use xanthates for metal separation by flotation process. The generation of these insoluble residues is common in all types of metallurgical complexes such as those from the zinc production by hydrometallurgical processes (leaching with H_2SO_4), which represent an economically attractive product for their treatment, when the production of these wastes is a function of the metallic content of the concentrates used in the leaching stages. Dutrizac[1] characterized a typical zinc concentrate used in a electrolytic plant, where amounts of Ag, Pb, and Cu were about 250 ppm, 0.56 wt pct, and 0.76 wt pct, respectively. Scott and Dienstbach[2] reported that in the case of a zinc refining plant, 5 ton of residues were produced for every 100 ton of calcine fed to the circuit. Residues contain several

D.M. ÁVILA-MÁRQUEZ is with the Instituto de Metalurgia-Facultad de Ingeniería, Universidad Autónoma de San Luis Potosí, Av. Sierra Leona 550, Lomas 2a sección, 78210 San Luis Potosí, San Luis Potosí, Mexico. I.A. REYES-DOMÍNGUEZ, J. AGUILAR-CARRILLO, and E.J. GUTIÉRREZ-CASTAÑEDA are with the Instituto de Metalurgia-Facultad de Ingeniería, Universidad Autónoma de San Luis Potosí and also with Catedrático CONACyT - Consejo Nacional de Ciencia y Tecnología, Colonia Crédito Constructor Del. Benito Juárez, 03940 Ciudad de México, Mexico. Contact e-mails: iareyesdo@conacyt.mx; alejandro.reyes@uaslp.mx A. BLANCO-FLORES is with the División de Mecánica, Tecnológico de Estudios Superiores de Tianguistenco, Carretera Tenango-Marquesa km 22, Santiago Tilapa, 52650 Santiago Tianguistenco, Estado de México, Mexico. Contact e-mails: blancoflores81@hotmail.com; alien.blanco@test.edu.mx H.P. TOLEDO-JALDIN is with the Facultad de Química, Universidad Autónoma del Estado de México, Paseo Tollocan y Paseo Colon, 50110 Toluca, Estado de México, Mexico. G. LÓPEZ-TÉLLEZ is with the Centro Conjunto de Investigación en Química Sustentable UAEM-UNAM, (CCIQS), Carretera Toluca-Atlacomulco Km 14.5, Unidad El Rosedal, 50200 Toluca, Estado de México, Mexico.

Manuscript submitted May 25, 2018.

Published online: 15 November 2018

metallic species with economical value such as Ag, Pb, Cu, Zn, among others. These species are present in different phases, mainly as sulfides (Ag_2S, $(Ag, Cu)_2S$, CuS, Cu_2S, ZnS), sulfates ($PbSO_4$), and oxides ($Zn_xFe_{3-x}O_4$).[3]

The concentration of copper by flotation processes requires the use of several reagents, added to the process to increase efficiency. Among the many types of collectors used in the flotation process, xanthogen formates and xanthic esters constitute a very important category. Xanthogen formates are synthetized by reacting xanthate with alkyl chloroformate, whose alkyl groups can vary with the chain length.[4] They have the capability of increasing the flotation of copper, zinc, and others metallic sulfides, due to their higher stability in acidic and basic media.[5] Ackerman *et al.*[4] found that xanthogens are more stable and effective for copper sulfide adsorption at a range of pH 5.0 to 10.0; however, adsorption at pH lower than 5.0 has not been reported in the literature.[6] Stability at a lower pH becomes very important considering the fact that it is not necessary to neutralize the acid residues of the leaching process, in contrast they can also be used for the recovery of metals by flotation.[7] Additionally, the affinity between S and O atoms of xanthate derivatives and Cu atoms from minerals is stronger than in the case of others collectors such as xanthates.

However, there is no information available in the literature regarding the influence of the structure of xanthate derivatives on their interactions with minerals, interactions established through an adsorption process specifically. The surface adsorption of mineral collectors is significant in flotation and concentration processes because the interfacial region of this biphasic system is governed by many interactions that involve several variables such as pH, adsorbent dose, temperature, or structure of collector molecules.[8] Molecular and mineral surface characteristics determine the interaction forces responsible for the adsorption and their effect on solid–liquid interfacial properties such as surface charge and hydrophobicity.[9] Therefore, it is important to understand the mechanism and characteristics of xanthate derivatives adsorption of sulfide minerals, because adsorption interactions may improve the selective separation of metals from the mineral and give a better understanding of the main mechanism between collector and mineral. Furthermore, the adsorption method provides information about contact time and maximum adsorption capacity, and while these type of studies have been conducted for xanthate collectors, they have not yet been carried out for compounds derived from xanthate.[10]

Nowadays, xanthate compounds are used as collectors in the flotation concentration process of valuable species. Some xanthate derivatives, such as xanthogen formates and xanthic esters have a high stability in acid medium and therefore, they can be considered as promising candidates not only to replace conventional collectors, but also to be used in concentration processes that involve highly acidic pH working conditions. There have been reported some investigations related to the interaction of xanthogens with mineral sulfides; however, the efficiency of these collectors has been only examined at neutral and basic pH conditions.[1] Several hypotheses have been proposed to describe the possible mechanisms of the interaction between xanthogens and minerals; however, they have not been supported with experimental results. The XPS technique is a powerful tool that allows validating the hypotheses that other authors have proposed regarding the adsorption mechanisms. Besides the facility to establish the bases of the mechanism, it is also possible to determine with precision and accuracy the interactions between the minerals and the organic groups of the collectors. It may settle the bases for future work to modify the surface of minerals or even to modify the structure of the collectors in order to improve the percentages of recovery, either from metals present in ores or in other sources such as acid leaching residues.

In the present research, isobutyl xanthogen ethyl formate and *O*-pentyl *S*-2-propenyl ester were used to investigate their interactions with copper sulfide mineral, in order to determine the mineral affinity. The influence of functional groups and chain length of two xanthate derivatives in the adsorption mechanism was evaluated through kinetics and adsorption experiments, being the adsorption process of collectors analyzed by FTIR and XPS techniques.

II. EXPERIMENTAL SECTION

A. *Reagents and Instruments*

Isobutyl xanthogen ethyl formate (C-4940) and *O*-pentyl *S*-2-propenyl ester (C-4410), with purities higher than 90 pct, were used as collectors in the present work. The molecular structures of the studied collectors are represented as in Figure 1.

Collectors were obtained from SNF Flomin™ mining reagent suppliers. Synthetic copper sulfide (CuS) was used as a stand-in for the mineral covellite and was acquired from Sigma-Aldrich Company (99 pct purity).

Phases were identified by X-ray diffraction (XRD) in a 2θ range of 0 to 90 deg, using a Bruker D8 Advance

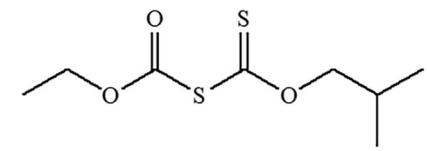

Isobutyl xanthogen ethyl formate (C-4940)

(a)

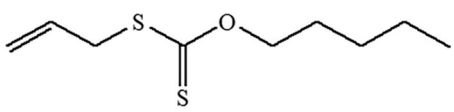

O-pentyl S-2-propenyl ester (C-4410)

(b)

Fig. 1—Molecular structure of collectors: (*a*) C-4940 and (*b*) C-4410.

X-ray diffractometer; equipped with a CuK radiation source and SOL-X solid-state detector.

Analysis included 2θ steps with a counting time of 0.3 seconds. Mineral phase identification was made with the ICDDPDF-2/4 database using the Diffrac. EVA V4.2.1 diffraction software. Fourier Transform Infrared Spectroscopy technique (FTIR) was used to analyze the two xanthate derivatives and the mineral before and after adsorption, to characterize the surface interactions between them. It was recorded in the 4000 to 400 cm^{-1} region with a Thermo Scientific Nicolet iS10 infrared spectrophotometer.

The experiments for the pH at the point of zero charge (pH_{pzc}) were carried out according to Blanco-Flores *et al.*[11] using a Thermo Scientific Orion Star A325 pHmeter. The UV/Vis technique was used to quantify the xanthate derivatives adsorbed on mineral surface at 284 and 274 nm for C-4410 and C-4940, respectively. The UV/Vis spectrum was obtained in a Thermo Scientific Genesys 10S UV/Vis spectrophotometer. The wide and narrow spectra of XPS were acquired using a JEOL JPS-9200, equipped with a Mg X-ray source (1253.6 eV) at 200 W, an area of analysis of 3 mm^2, a pass energy of 15 eV, and a vacuum of the order of 7.5×10^{-9} Torr for all samples. The spectra were analyzed using the Specsurf™ software included with the instrument; all spectra were charge corrected using the adventitious carbon signal (C1s) at 284.5 eV. The Shirley method was used for the background subtraction, whereas curve fitting employed the Gauss–Lorentz method.

B. *Kinetic Adsorption Experiments*

Kinetic adsorption experiments were performed for determination of the time required for the mineral surface hydrophobization. The experimental set-up required batch experiments, at an initial xanthate derivative concentration of 20 mg g^{-1}, adding a dose of covellite and 35 mL of xanthate derivative solution. The mixture was blended at room temperature at 400 rpm using a magnetic stirrer. The covellite was then separated by filtration to determine the fraction of non-adsorbed xanthate derivatives in each experiment.

To study the effect of covellite dose on adsorption of both xanthate derivatives, the values of doses for the different experiments were 10, 30, 50, 70, 90, 100, and 300 mg. To study the effect of pH in the xanthate derivative solutions, pH was adjusted from 2 to 6 using 0.1 mol L^{-1} HCl and 0.1 mol L^{-1} NaOH solutions. All experiments were carried out at room temperature and were performed in duplicate for C-4410 and C-4940 xanthate derivatives.

C. *Isothermal Adsorption Experiments*

One dose of covellite was put in contact with 35 mL of solution at different initial concentrations of xanthate derivatives ranging from 5 to 45 mg L^{-1} for any time period above to equilibrium time, obtained from the kinetic experiments at room temperature determined separately for both xanthate derivatives. The mixture was afterwards filtered to determine the non-adsorbed amount of xanthate derivatives. These experiments were performed by duplicate.

For all experiments of kinetic and isothermal adsorption, the pH solution values were measured before and after the process with an Orion 3-Star pH meter equipped with a Thermo Ultra-Sure flow electrode, which has a reading pH range of 0 to 14 ± 0.01 at a maximum temperature of 100 °C. The adsorbed amount of xanthate derivatives (q) at time (mg g^{-1}) was determined from Eq. [1]:

$$q = \frac{(C_i - C_t)}{m} \cdot V, \qquad [1]$$

where C_i (mg L^{-1}) is the initial xanthate derivative concentration, C_t (mg L^{-1}) is the concentration of the solution at time t, V (L) is the volume of xanthate derivative solution, and m (g) is the dose of covellite.

III. RESULTS AND DISCUSSIONS

A. *Evaluation of Xanthate Derivatives Stability in Aqueous Solution*

To evaluate the stability of the xanthate derivatives used in this investigation, several samples of the collectors were placed in aqueous solution at different conditions of pH and time. The residual concentration was determined by UV/Vis spectrometry.

Both collectors obeys the Beer´s law, showing linearity until concentrations of about 70 mg L^{-1}. Likewise, the wavelengths of maximum absorption were 284 and 274 nm for collectors C-4410 and C-4940, respectively. As it is observed in Figure 2, the intensity of C-4410 collector is almost constant in the evaluated pH range (2 to 6). Additional signals that indicate the existence of other species were not observed under the investigated conditions, even at higher pH values (8 and 10). On the

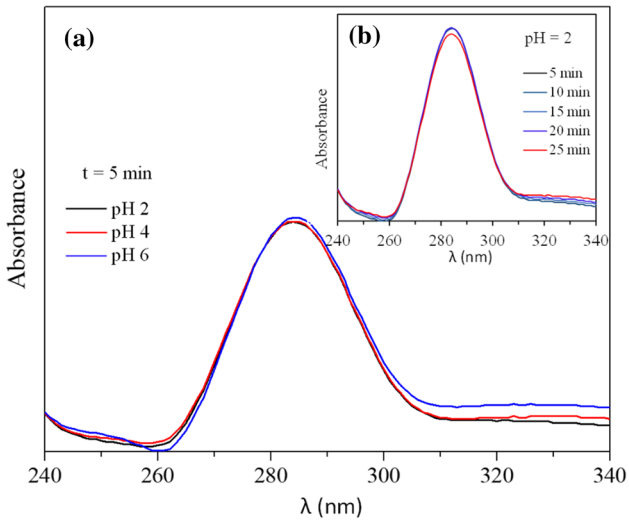

Fig. 2—Evaluation of stability in aqueous solution of collector C-4410, [C-4410] = 30 mg L^{-1}, T = 25 °C, as a function of: (*a*) pH; (*b*) contact time with water.

other hand, according to Figure 2(b), the C-4410 collector shows a slight degradation after 25 min in aqueous solution, being much longer than the acceptable time of pulp conditioning in a typical flotation process (5 minutes). Likewise, prolonged conditioning times could have negative effects on the flotation process. A similar behavior was found in the case of C-4940 collector under the same conditions (Figure 2), but for higher pH values (8 and 10) were observed two spectroscopically distinct species present at 226 and 301 nm, which indicate the instability of C-4940 collector at higher pH values. According to Fairthorne,[12] these two species can be assigned to the basic and acidic form of the collector.

B. *Characterization*

Figure 3 shows the XRD pattern corresponding to synthetic copper sulfide (covellite). As can be seen, the main reflections of this phase are in agreement with PDF 00-006-0464, which confirms the information provided by suppliers of the synthetic mineral. Additional signals of other phases are not observed in the XRD pattern confirming the presence of a pure phase.

The FTIR spectra obtained from the pure xanthate derivative, copper sulfide, and xanthate derivative + copper sulfide at pH 2 are shown in Figures 4(a) and (b); the main bands of absorption are included in this figure. Spectrums of C-4410, copper sulfide without treatment, and C-4410 + copper sulfide are presented Figure 4(a). The most intense signals that appear at 1050 and 1208 cm^{-1} are related to the asymmetric and symmetric stretching of the C-O-C bond, respectively, of the ester functional group. The weakest signals observed at 920, 985, and 1464 cm^{-1} belong to the stretching of the C-S bond, in addition, the signal at $\approx$ 736 cm^{-1} is related to the stretching of the C-S-C bond. At 1638 cm^{-1}, it is possible to observe the stretching of the C=C from the propenyl group, while signals observed at 2960, 1377, and 1464 cm^{-1} belong to the stretching of the C-H, -CH_2-, and -CH_3 bonds.[13]

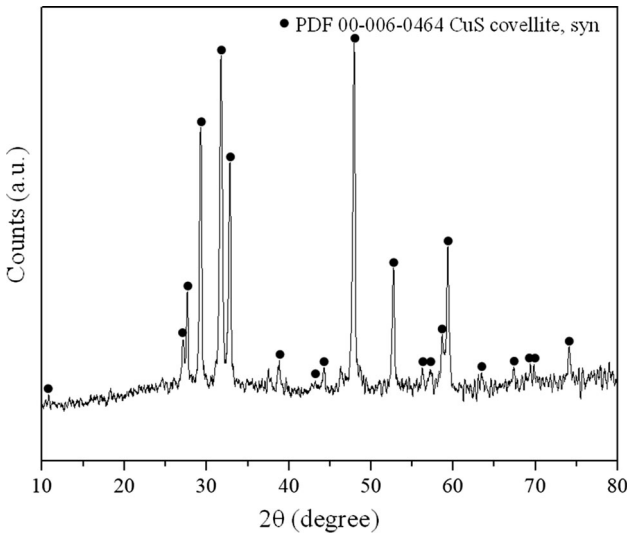

Fig. 3—X-ray pattern corresponding to synthetic copper sulfide.

The spectrum of C-4940 is shown in Figure 4(b), in this case, the most intense signals observed at 1745 and 1025 cm^{-1} are related to the C=O bond from the formate group. Signals at 1127 and 1265 cm^{-1} relate to the asymmetrical and symmetrical stretching of the C-O-C bond, respectively, and the weak signal at 774 cm^{-1} is due to the stretching of the O-(C=O)- group (formate). Signals at 2965, 1468, and 1375 cm^{-1} are characteristic vibration modes from the C-H, -CH_2-, and -CH_3 bonds, respectively.[13]

In the case of the copper sulfide spectrums, there are no intense signals due to the fact that this compound does not absorb in the range of 4000 to 500 cm^{-1}, the CuS signals can only be observed at values less than 400 cm^{-1}.[14]

Regarding the copper sulfide spectrums treated with xanthate derivatives at pH 2 presented in Figure 5 (approach of the zones marked in Figures 2(a) and (b), it can be observed that the main signals of the collector are slightly shifted. This indicates that the adsorption of xanthate derivative on the copper sulfide surface has occurred. These absorption bands are related with the -O-C(=S)-, C=S y –O-C=O groups and correspond to the adsorption sites on the copper sulfide surface. In the case of C-4410 + CuS (Figure 5(a)), the bands observed at 920, 1058, and 1212 cm^{-1} correspond to the principal signals observed in the spectrum of pure C-4410 (Figure 4(a)). While the signals in the spectrum of C-4940 + CuS (Figure 5(b)) at 845, 960, 1030, 1130, 1265, and 1745 cm^{-1} correspond to principal signals observed in the spectrum of pure C-4940 (Fig. 4(b)). Additional signals are observed and they are related to the Cu-O interaction on the copper sulfide surface. In both spectrums of xanthate derivative + CuS, it is possible to observe signals at $\approx$ 2165, 2110, 2040, 1982, and 1700 cm^{-1} that correspond to the C-O interaction with Cu^{2+} cations.[13,15] Additionally, the strong band at $\approx$ 1520 cm^{-1} along with other signals with low intensity are probably related to precipitation of $CuCO_3$ on the surface of the treated copper sulfide, and the unidentified signals are related with other C-O interactions, which is consisting with the results of Busca.[15]

XPS studies on copper sulfide conducted before and after adsorption process for C-4410 and C-4940 collectors revealed that the mineral interacted with both collectors through C=S and C=O functional groups. Covellite was identified by the Cu $2p^{3/2}$ spectrum at 934.84 eV. The presence of two peaks at 159.92 and 161.63 eV is attributed to CuS, and S^{2-}, and S_2^{2-} bonds, respectively (Figures 6(a) and (b)). This is consistent with the complex structure of covellite.[16]

The XPS results of C-4410 adsorption by covellite show that Cu atoms are preferentially bonding to –S sites although the interaction Cu–O could have also taken place (Figures 7(b) and (c)). The latter interaction is clearly recorded in the signals of the O 1s spectrum (Figure 7(d)), where a signal corresponding to C-O groups is also registered.[17] These interactions are complemented by the signals in the C 1s spectrum[18]

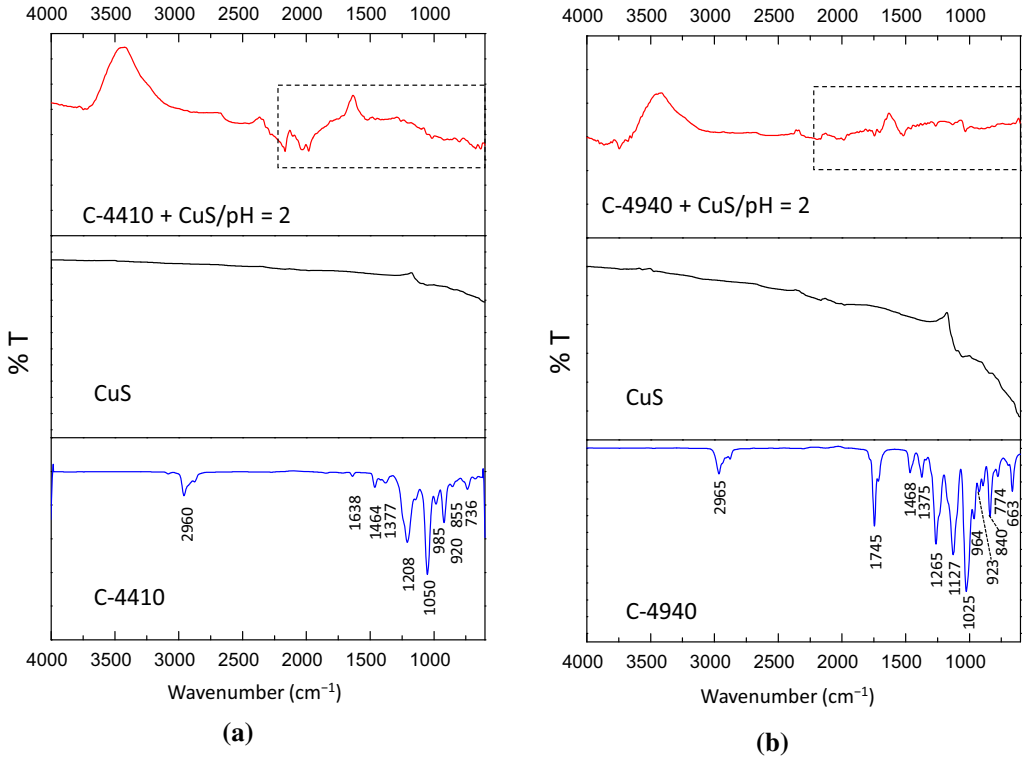

Fig. 4—FTIR spectrums of pure xanthate derivative and copper sulfide before and after adsorption: (*a*) C-4410 and (*b*) C-4940; pH 2, (xanthate derivative) = 30 mg L^{-1}, and contact time t = 5 min.

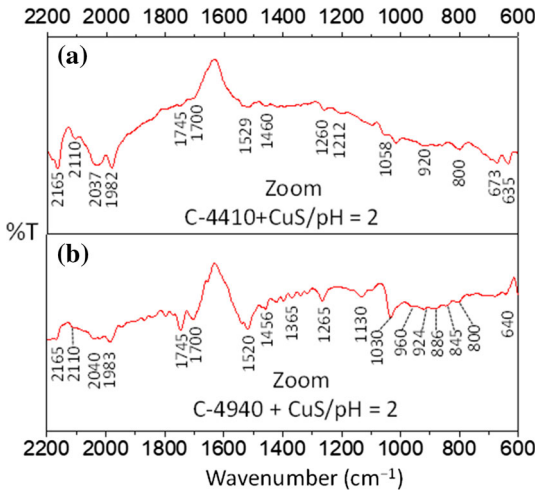

Fig. 5—FTIR spectrums of xanthate derivative + CuS (approach of the areas marked in Figs. 4(a) and (b): (*a*) C-4410 and (*b*) C-4940.

that shows the interactions between the groups constituting C-4410 (Figure 7(a)).

In the case of C-4940 adsorption, the spectra are similar to those of C-4410 adsorption, with the main difference related to the presence of two functional groups -C=S and -C=O,[19] necessary to achieve Cu interaction (Figures 8(a) through (d)).

These results suggest a mechanism of interaction between covellite and xanthogen when the adsorption took place.

C. *Kinetic Adsorption Experiments*

1. *Effect of covellite dose*

The dose of covellite selected for adsorption experiments was 0.05 g (Figure 9). With a higher amount, the adsorption of C-4940 and C-4410 collectors may decrease due to a mass transfer resistance increase or because the fine powder could agglomerate causing the reduction of surface area and blockage of the adsorption sites.[20] Besides, the hydrophobicity of the mineral may be reduced.

2. *Effect of pH of the xanthate derivative solutions*

The equilibrium time for each adsorption process was different. The obtained equilibrium times at pH 2, 4, and 6 were for C-4410 12, 12, and 20 minutes; and for C-4940 were 9, 12, and 30 minutes, respectively. The shortest time was achieved for C-4410 adsorption at pH 2 and 4. For C-4940 adsorption, the shortest time was achieved at pH 2 followed by pH 4. The adsorption at pH 6 for C-4410 and C-4940 required more time, probably due to the hindrance a higher pH creates for the molecule to reach the adsorption sites. In general terms, the obtained equilibrium times are in accordance with the conditioning times for a typical flotation process.[21]

The adsorbed amount of xanthate derivative for the different pH values also showed significant differences (Figures 10(a) and (b)). For both xanthate derivatives, the adsorption increases with time from the initial contact between mineral and xanthate derivative solutions. This is very important since flotation is the next

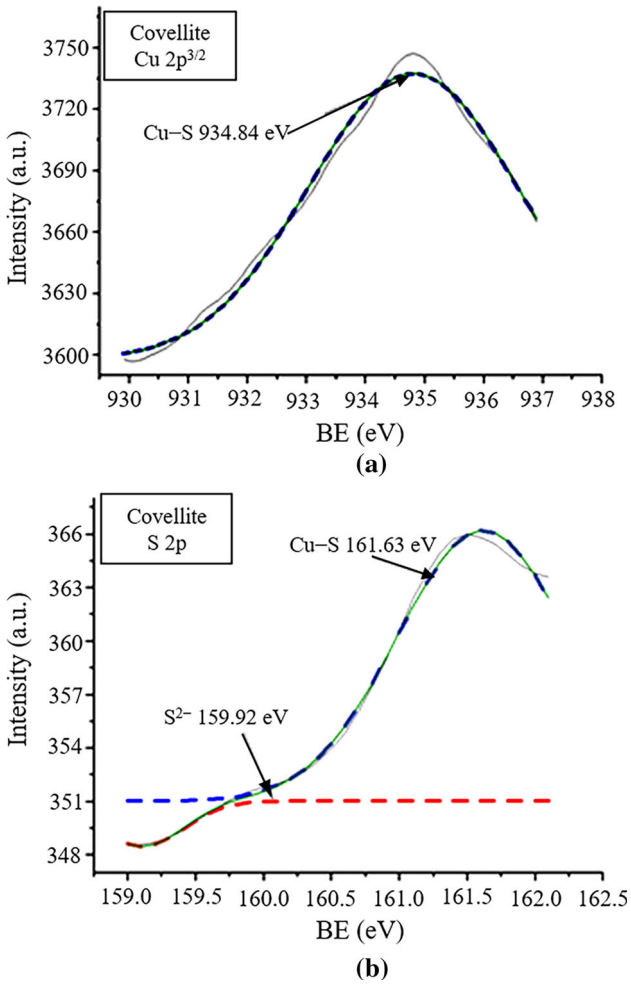

Fig. 6—XPS spectrum of covellite before adsorption: (*a*) Cu $2p^{3/2}$ and (*b*) S 2p.

stage in the metal recovery process and it requires a lower contact time between mineral and collector. In Figure 10(a), the adsorption of C-4410 shows a marked difference between the three values of pH, being higher at pH 6. This behavior is in concordance with the findings reported by other authors. They stated that xanthogens are effective as copper sulfides collectors in a wide range of pH values from 5 to 10.5.[22] In contrast, the C-4940 adsorption process is favored at pH 2 (Figure 10(b)), although the difference is small at pH 6 for a longer contact time. This is probably due to the presence of carboxylic groups in C-4940 that improve adsorption since these functional groups act as alternative sites for bonding with the covellite.

Therefore, the C-4410 xanthogen can be used as a collector in a wide range of pH but C-4940 xanthic ester is limited to less acidic pH according to the UV/Vis results. However, the equilibrium time at pH 2 and 4 in all experiments was similar. The subsequent flotation process could be carried out at the same contact time but the use of a particular collector will depend on the pH of medium.

Since the main objective of the present research was to assess the effectiveness of collectors at acidic pH, they were used the experimental data for pH 2 in the subsequent steps. Thus, the pseudo first- and pseudo second-order kinetic non-linear models[23] were applied to experimental data for pH 2 for C-4410 and C-4940 adsorption (Table II).

The pseudo first-order model is commonly used for homogeneous sorbents and physical adsorption, where the adsorption rate is proportional to the solute concentration. The experimental kinetic data could be adjusted to the following Eq. [2]:

$$q_t = q_e(1 - e^{kt}), \qquad [2]$$

where q_t and q_e are the amounts of collector adsorbed (mg g^{-1}) in the equilibrium and at time t (minutes), respectively, and k (min^{-1}) is the adsorption rate constant of the pseudo first-order model.

The pseudo second-order model can be represented by Eq. [3], where the rate-limiting step is the surface adsorption that includes chemisorption, involving valence forces through the sharing or exchange of electrons between covellite and xanthate derivatives.

$$q_t = \frac{q_e^2 t k_2}{1 + q_e t k_2}, \qquad [3]$$

where q_t and q_e are the amounts of collector adsorbed (mg g^{-1}) in the equilibrium and at time t (min), respectively, and k_2 (g mg^{-1} min^{-1}) is the adsorption constant of pseudo first-order rate constant. The obtained kinetic model parameters for C-4410 and C-4940 adsorption onto covellite are shown in Table II.

q_{eexp} and q_{ecal} values are similar for the pseudo first-order model, and the statistic parameters values had a better fit for the pseudo first-order model results. Both aspects indicate that experimental data have a slightly better fitted for the pseudo first-order model than pseudo second-order model for C-4410 adsorption. Therefore, the C-4410 adsorption probably takes place through a non-covalent interaction process that involves electrostatic and van der Waals (Cu-π electron) interactions (Figure 11). Since pH_{zpc} (6.05) is higher than pH solutions after C-4410 adsorption (pH_f 2.12), the surface is positively charged and electrostatic interactions are present.

The best fit for C-4940 adsorption was achieved for the pseudo second-order model, which means that the interaction was through a chemisorption process. This is consistent with the results obtained from the comparison between covellite pH_{zpc} and pH_f (2.17) for the C-4940 adsorption process, because the surface is charged positively. Moudgil *et al.*,[24] consider the electrostatic interaction to be less important for flotation purposes (Figure 11). Therefore, the adsorption of C-4410 is less feasible than C-4940 for later stages of flotation minerals. The information obtained from the kinetic models allowed to propose the mechanism of the covellite-collectors interaction (Figure 11), which is in agreement with the results obtained from XPS analyses

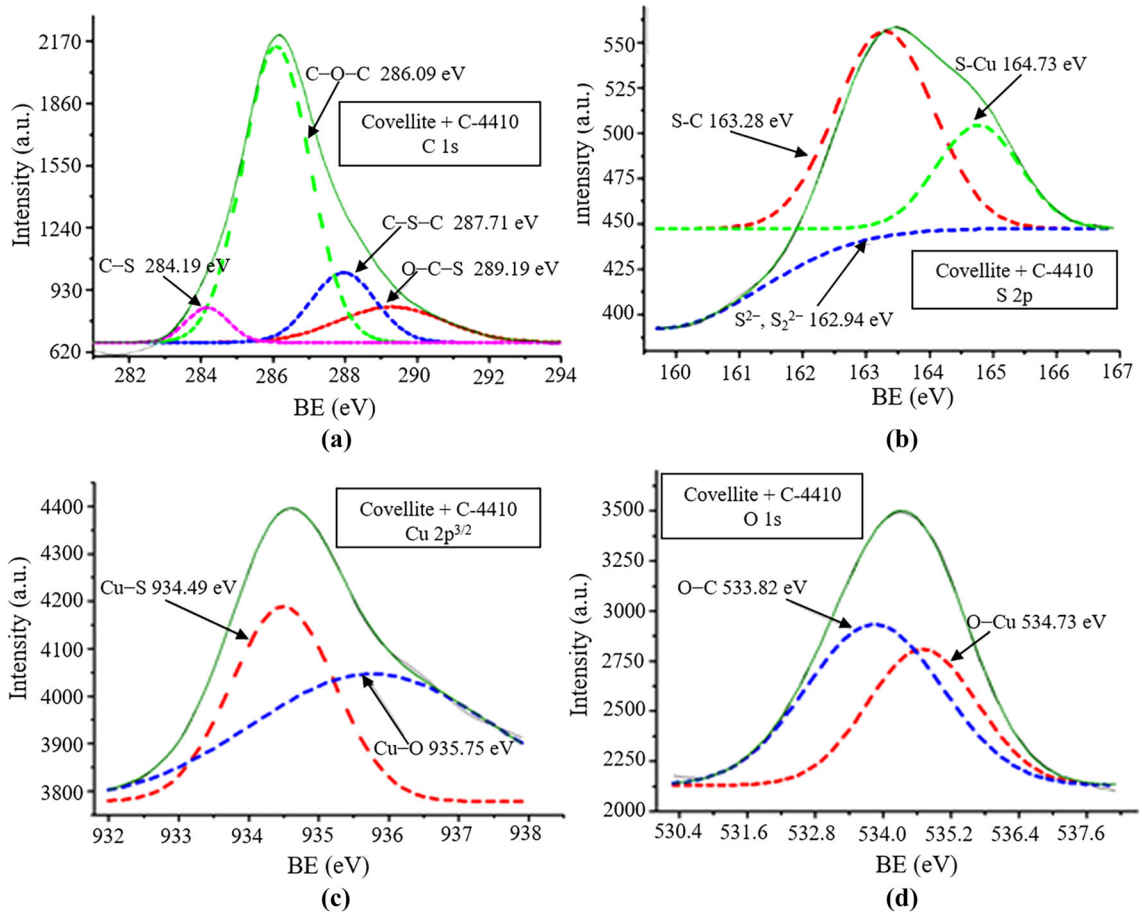

Fig. 7—XPS spectra of covellite after xanthate derivative: (*a*) C 1s, (*b*) S 2p, (*c*) Cu $2p^{3/2}$, and (*d*) O 1s.

of covellite, and C-4410 and C-4940 adsorption on mineral (Figures 6 through 8).

D. *Isotherm Adsorption Experiments*

The experimental data obtained from the isotherms were used to apply Langmuir, Freundlich, Langmuir–Freundlich, Temkin, Redlich–Peterson, and Dubinin–Radushkevich non-linear models.[25,26] These isotherm models are the most frequently used for liquid/solid adsorption systems (see Table I).

The better-fit models for C-4410 and C-4940 adsorption were Redlich–Peterson and Freundlich model, respectively (Table II). However, the value of $b_{rC\text{-}4410}$ is closer and describes an isotherm similar to that of the Freundlich model.[30] The value of $1/n$ for both adsorption processes (0.40 and 0.37, respectively) was between 0 and 1 indicating favorable processes. The heterogeneity was higher for C-4940 than C-4410 adsorption, probably related to the different functional groups on the C-4940 xanthic ester molecule (Figure 10), meaning that for C-4940, the adsorption preferentially occurred on heterogeneous surfaces. From the Temkin constant (*B*) a factor (*b*) was obtained related to adsorbent–adsorbate interactions. The C-4410-covellite interaction (244.62) was lower than C-4940-covellite (313.53) interaction.[31]

The maximum adsorption capacity was 57.07 and 44.62 mg g^{-1} for C-4410 and C-4940, respectively. Such values could be explained as derived from the dimensions of the xanthate derivative molecules. The C-4410 molecule (14.49 × 5.51 Å) is smaller than the C-4940 molecule (14.38 × 7.18 Å) and this could favor the existence of a steric impediment between large molecule and the distributions of adsorption sites. The values of "b_r" parameters from Redlich–Peterson model confirm this idea.[23] Therefore, both selected organic compounds are potential collectors for copper recovery in an acid flotation process.

E. *Microflotation Tests*

Microflotation tests with synthetic copper sulfide were not possible to carry out since the particle size is extremely fine, therefore it was decided to conduct microflotation tests with a natural massive sample of Cu mineral. The sample was obtained from the Santa Maria de la Paz mine localized in San Luis Potosi, Mexico. Elemental chemical analysis show high copper and iron contents, 40.4 and 12.3 wt pct, respectively. According

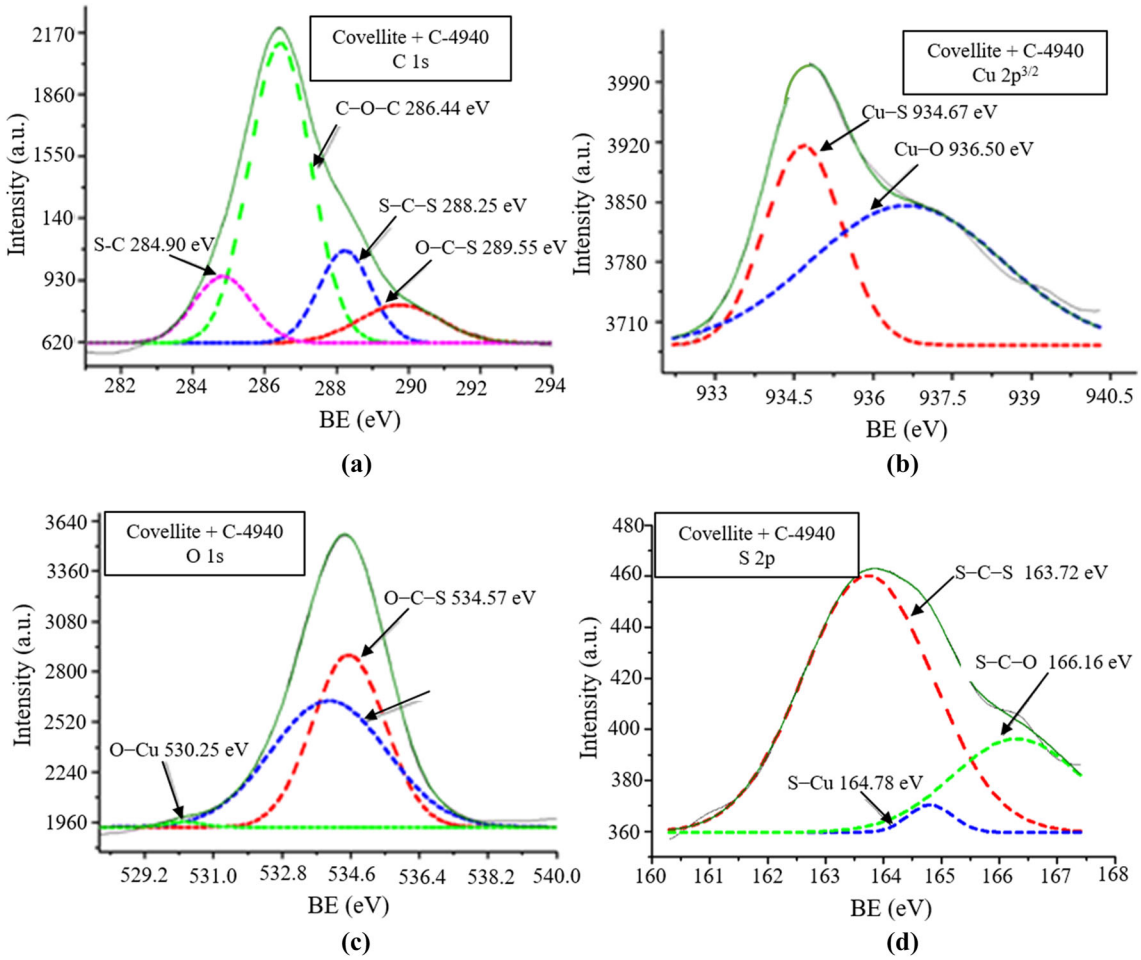

Fig. 8—XPS spectrum of covellite after xanthate derivative (*a*) C 1s, (*b*) Cu $2p^{3/2}$, (*c*) O 1s, and (*d*) S 2p.

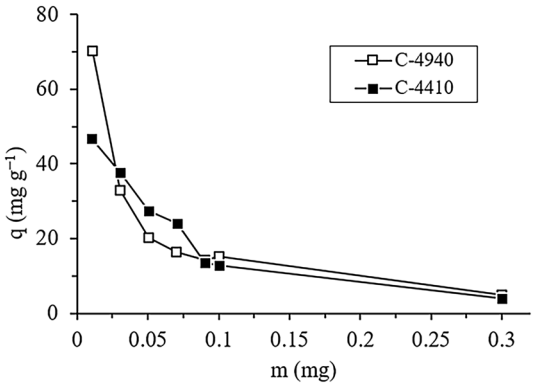

Fig. 9—Dose of covellite for C-4940 and C4410 adsorption.

to results of XRD, the sample is mainly constituted for chalcopyrite and bornite, and to a lesser extent for covellite. The mineral sample was grounded using a porcelain mortar and then sieved; the particle size used for microflotation tests was the one retained in the 325 mesh. For every microflotation test, 100 mL of deionized water, 1 g of Cu mineral, and the collector solution needed to adjust a concentration of [C-4410] = 20 mg L^{-1}, were simultaneously added. The pulp was conditioned for 5 minutes and pH was kept constant.

The pulp was then transferred to a Hallimond tube, bubbling pure N_2 at a flow of 8 mL min^{-1}. After 1 minute of bubbling, the products were collected by filtration, dried, and weighed for later determination of Cu. It was determined *via* atomic absorption spectroscopy in a PerkinElmer AAnalyst 200 spectrometer. Results of the microflotation tests are presented in Figure 12.

Considering that C-4410 collector showed higher stability in a wide range of pH, based on the UV/Vis analysis, there are only presented the results obtained for this collector. Figure 12 shows the recovery of Cu at pH values of 2, 4, 6, 8, and 10. As can be seen, at pH 2, the collector exhibits a Cu recovery of 53 pct; with increments in pH, the recovery increases up to at pH 10 it is about 84.01 pct. In general, it is observed that the collector C-4410 has an excellent response in both acidic and alkaline medium. Although the recovery for pH 2 can be considered as acceptable, it is possible to improve

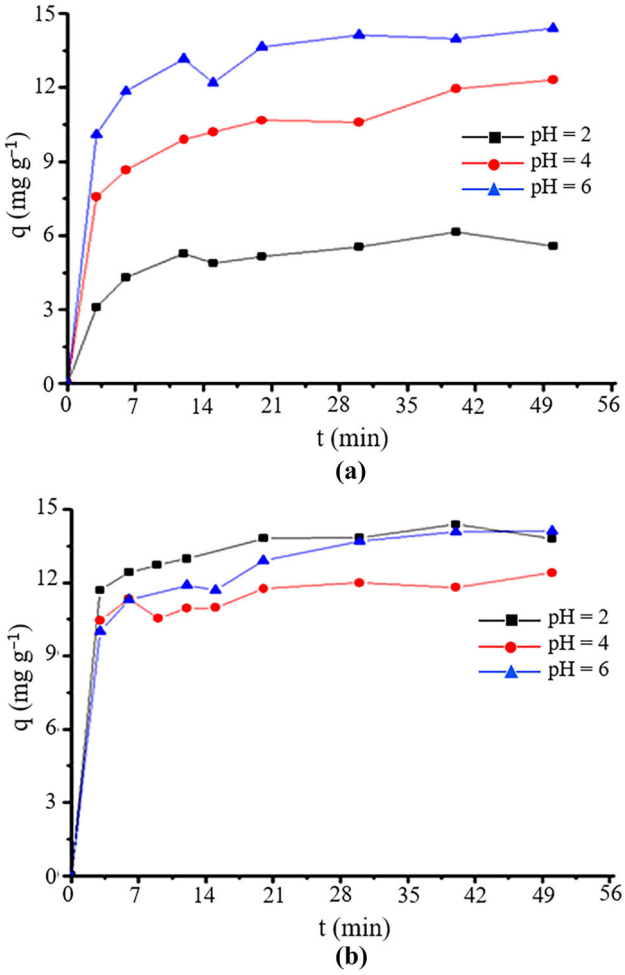

Fig. 10—Kinetic adsorption on covellite mineral for different pH values: (*a*) C-4410 and (*b*) C-4940 xanthate derivative solutions.

the efficiency by varying the flotation variables. This observation is consisting with the data reported by Ackerman *et al.*,[32] who obtained similar results using isopropyl xanthogen ethyl formate in the flotation of copper sulfides (chalcopyrite, chalcocite, bornite, and covellite) at different pH conditions (5.5 to 10.5).

IV. CONCLUSIONS

The collectors C-4940 and C-4410 have functional groups distinguished by their marked affinity for the Cu contained in the covellite. The adsorption of both xanthate derivatives was confirmed by FTIR and XPS analyses. XPS results indicate the actuality of Cu-S interaction in C-4410 adsorption, and Cu-S and Cu-O interaction in C-4940 adsorption. The equilibrium time for each adsorption process was different. The adsorption of the C-4410 collector showed a marked difference between three values of pH being higher at pH 6. In contrast, the C-4940 adsorption process is favored at pH 2 but the difference is small at pH 6 for a longer contact time. The C-4410 xanthogen can be used as collector in a wider range of pH but C-4940 is limited at acidic pH. The C-4410 adsorption process occurs through non-covalent interaction processes that involve electrostatic and van der Waals interactions, while the C-4940 adsorption was achieved through a chemisorption process. The better-fit isotherm adsorption models for C-4410 and C-4940 adsorption processes were Redlich–Peterson and Freundlich model, respectively. For C-4940, the adsorption process occurs on heterogeneous surfaces. The maximum adsorption capacities were 57.07 and 44.62 mg g^{-1} for C-4410 and C-4940, respectively.

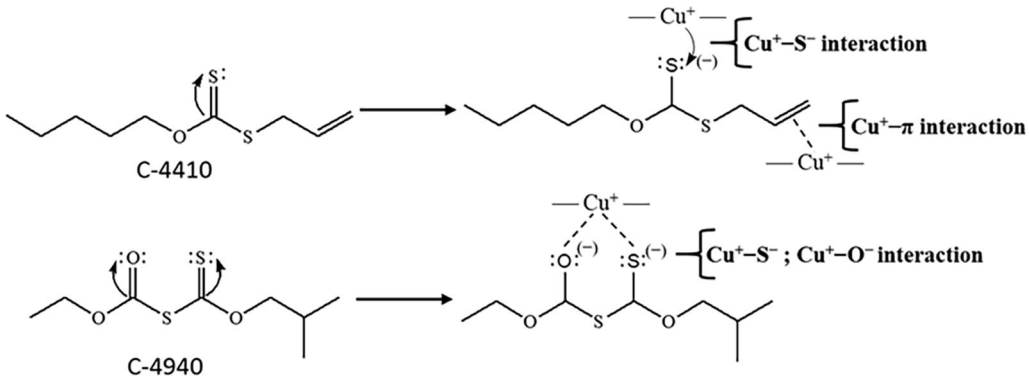

Fig. 11—Mechanisms of interaction for covellite mineral and xanthate derivative collectors.

Table I. List of Adsorption Isotherm Models Used in the Evaluation of Covellite-Xanthate Derivatives Interaction

Isotherm Models	Non-linear Equation	Description Parameters	Description of Models
Langmuir	$q_e = \frac{K_L q_{max} C_e}{1+C_e K_L}$	q_{max}: maximum adsorption capacity (mg/g) K_L: constant related to the free energy of adsorption (L g^{-1})	the model assumes uniform adsorption energies on the homogeneous adsorbent surface[27]
Freundlich	$q_e = K_F C_e^{1/n}$	K_F: constant indicative of the relative adsorption capacity of the adsorbent (mg g^{-1}) (mg $L^{-1})^n$. $1/n$: indicates the intensity of the adsorption	the Freundlich isotherm is an empirical equation suited for heterogeneous surfaces[27]
Langmuir–Freundlich	$q_e = \frac{K C_e^{1/n}}{(1+a C_e^{1/n})}$	K and a are empirical constants	this model is a combination of both Langmuir and Freundlich models[11]
Temkin	$q_e = \frac{RT}{B} \ln(A C_e)$	B: Temkin constant which is related to the heat of sorption (J mol^{-1}) A: Temkin isotherm constant (L g^{-1})	the model is based on the adsorbent–adsorbate interaction on adsorption isotherm[28]
Redlich–Peterson	$q_e = \frac{K_r C_e}{1+a_r C_e^{b_r}}$	K_r: Redlich–Peterson constant (L mg^{-1}) a_r: constant (L mg^{-1}) b_r: exponent between 0 and 1	this model is an empirical isotherm. the mechanism of adsorption does not follow ideal monolayer adsorption[29]
Dubinin–Radushkevich	$q_e = q_s e^{-K_D \varepsilon^2}$	K_D: Dubinin–Radushkevich isotherm constant (mol^2 kJ^{-2}) ε: characteristic energy of adsorption (kJ mol^{-1}) q_s: theoretical saturation capacity (mg g^{-1})	this isotherm describes the adsorption mechanism with a Gaussian energy distribution onto a heterogeneous surface[27]

q_e: amount of solute adsorbed per unit weight of adsorbent at equilibrium (mg g^{-1}), C_e: equilibrium concentration of solute in bulk solution (mg L^{-1}).

Table II. Kinetic and Isotherm Model Parameters for C-4410 and C-4940 Adsorption on Covellite

Parameters/Collector	C-4410	C-4940
Kinetic model parameters		
Pseudo first order		
q_{eexp} mg g^{-1}	5.219	13.8037
q_{ecal} (mg g^{-1})	5.2658	12.7043
k (min^{-1})	0.2890	0.6153
R^2	0.9880	0.9820
RSS	0.2295	2.5303
χ^2	0.0459	0.3615
Pseudo second order		
q_{ecal} (mg g^{-1})	5.9697	14.1283
k_2 (g mg^{-1} min^{-1})	0.0656	0.0979
R^2	0.9879	0.9951
RSS	0.2300	0.6834
χ^2	0.04601	0.0976
Isotherm model parameters		
Langmuir		
q_{max} (mg g^{-1})	57.07	44.62
K_L (L g^{-1})	0.44	0.26
R^2	0.9572	0.9183
Freundlich		
K_F (mg g^{-1})/(mg L^{-1})^n	17.91	12.01
$1/n$	0.40	0.37
R^2	0.9781	0.9587
Langmuir–Freundlich		
q_{max} (mg g^{-1})	114.40	333.32
K_{LF} (L g^{-1})	0.19	0.04
$1/n$	1.82	2.51
R^2	0.9806	0.9551
Temkin		
A (L g^{-1})	7.93	4.91
B (J mol^{-1})	10.12	7.90
R^2	0.9584	0.9363
Redlich–Peterson		
K_r (L mg^{-1})	73.62	71.64
a_r (L mg^{-1})	3.02	5.04
b_r	0.71	0.68
R^2	0.9836	0.9566
Dubinin–Radushkevich		
q_{max} (mg g^{-1})	43.29	34.17
β (mol^2 J^{-2})	2.48×10^{-7}	4.61×10^{-7}
ε (kJ mol^{-1})	1.42	1.04
R^2	0.8332	0.7494

R^2 coefficient of correlation, RSS residual sum of squares, χ^2 Chi square.

ACKNOWLEDGMENTS

The authors would like to thank The National Council of Science and Technology (CONACYT by its Spanish acronym) of Mexico for the financial support granted through the project CB-254952-2016 and The Institute of Metallurgy of the Autonomous University of San Luis Potosi (IM-UASLP by its Spanish acronym) for the facilities to development the experimental work. Delia Ávila thanks the CONACYT for the postgraduate studies scholarship granted. The technical assistance of Francisco Galindo and Rosa Lina Tovar, from the IM-UASLP, and Nicolas Miranda from the Engineering Faculty of the UASLP is also recognized.

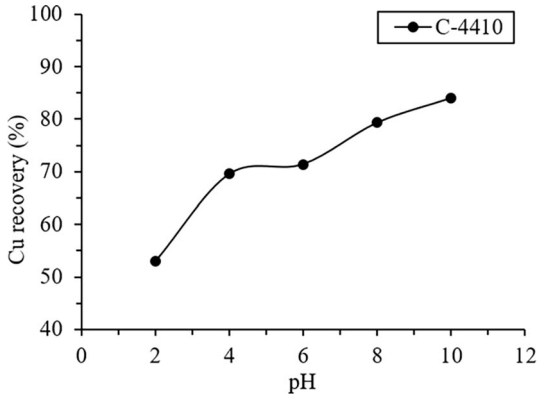

Fig.12—Cu recovery during flotation of a natural sample of copper sulfide. [C-4410] = 20 mg L^{-1}, conditioning time t = 5 min, flotation time t = 1 min.

REFERENCES

1. J. E. Dutrizac: *Proceedings of a World Symposium on Metallurgy and Environmental Control,* Sponsored by the TMS Lead, Zinc, and Tin Committee, 1990, vol. 11, pp. 161–91.
2. J.D. Scott and U. Dienstbach: in *IMM Conf. on Extractive Metallurgy*, 1990, pp. 121–34.
3. T.T. Chen and J.E. Dutrizac: *Metall. Trans. B*, 1988, vol. 19, pp. 803–17.
4. P.K. Ackerman, G.H. Harris, R.R. Klimpel, and F.F. Aplan: *Int. J. Miner. Process.*, 2000, vol. 58, pp. 1–13.
5. P. Somasundaran and M. B. Moudgil: *Reagents in Mineral Technology*, 21st ed., New York, N. Y., Marcel Dekker Inc., 1998, pp. 79–104.
6. J. Xiao, G. Liu, H. Zhong, Y. Huang, and Z. Cao: *J. Taiwan Inst. Chem. E.*, 2017, vol. 71, pp. 38–46.
7. L.C. Juncal, M.V. Cozzarín, and R.M. Romano: *Spectrochim. Acta A*, 2015, vol. 139, pp. 346–55.
8. F. Yang, W. Sun, and Y. Hu: *Miner. Eng.*, 2012, vol. 39, pp. 140–48.
9. P. Somasundaran and L. Zhang: *J. Petrol. Sci. Eng.*, 2006, vol. 52, pp. 198–212.
10. J. Xiao, N. Di, G. Liu, and H. Zhong: *Colloid. Surf. A*, 2014, vol. 456, pp. 203–10.
11. A. Blanco-Flores, A. Colín-Cruz, E. Gutiérrez-Segura, V. Sánchez-Mendieta, D.A. Solís-Casados, M.A. Garrudo-Guirado, and R. Batista-González: *Environ Technol*, 2014, vol. 35, pp. 1508–19.
12. G. Fairthorne, D. Fornasiero, and J. Ralston: *Int. J. Miner. Process.*, 1996, vol. 46, pp. 137–53.
13. G. Socrates: *Infrared and Raman Characteristics Group Frequencies-Tables and Charts*, 3rd ed., Wiley, Chichester, 2001, pp. 222–23.
14. R.O. Kagel and R.A. Nyguist*: Infrared Spectra of Inorganic Compounds-(3800-45cm^{-1})*. Academic Press, Inc, New York, N.Y., 1971, pp. 249–50.
15. G. Busca: *J. Mol. Catal.*, 1987, vol. 43, pp. 225–36.
16. N. Karikalan, R. Karthik, S.M. Chen, C. Karuppiah, and A. Elangovan: *Sci. Rep.*, 2017, vol. 7, p. 2494.
17. H. Tillborg, A. Nilsson, B. Hernnäs, N. Mårtensson, and R.E. Palmer: *Surf. Sci.*, 1993, vol. 295, pp. 1–12.
18. U. Gelius, P.F. Heden, J. Hedman, B.J. Lindberg, R. Manne, R. Nordberg, C. Nordling, and K. Siegbahn: *Phys. Scripta*, 1970, vol. 2, pp. 70–80.
19. M. El-Desawy: *Characterization and application of aromatic self-assembled monolayers* (Doctoral dissertation, University of Bielefeld), 2007.
20. J.O. Babalola, B.A. Koiki, Y. Eniayewu, A. Salimonu, J.O. Olowoyo, V.O. Oninla, V.O. Oninlac, H.A. Alabic, E.A. Ofomaja, and M.O. Omorogie: *J. Environ. Chem. Eng.*, 2016, vol. 4, pp. 3527–36.

21. S.M. Bulatovic: *Handbook of Flotation Reagents: Chemistry, Theory and Practice Flotation of Sulfide Ores*, vol. 1, 1st ed., Nueva York, NY, Elsevier Science; 2007, pp. 235–40.
22. L.C. Juncal: *Preparación, caracterización y estudio de las propiedades de compuestos xantatos y xantógenos con potenciales aplicaciones farmacológicas* (Doctoral dissertation, Facultad de Ciencias Exactas, Universidad de la Plata), 2014.
23. T.M. Berhane, J. Levy, M.P. Krekeler, and N.D. Danielson: *Chemosphere*, 2017, vol. 176, pp. 231–42.
24. B.M. Moudgil, H. Soto and P. Somasundaran: *Reagents in Mineral Technology*, New York, N. Y., Marcel Dekker Inc., 1988, pp. 79–104.
25. A. Verma, S. Kumar, and S. Kumar: *J. Environ. Chem. Eng*., 2017, vol. 5, pp. 2290–2304.
26. H.N. Tran, S.J. You, A. Hosseini-Bandegharaei, and H.P. Chao: *Water Res*., 2017, vol. 120, pp. 88–116.
27. M.L. Soto, A. Moure, H. Domínguez, and J.C. Parajó: *J. Food Eng*., 2011, vol. 105, pp. 1–27.
28. K.C. Nebaghe, Y. El Boundati, K. Ziat, A. Naji, L. Rghioui, and M. Saidi: *Fluid Phase Equilib*., 2016, vol. 430, pp. 188–94.
29. N. Ayawei, A.N. Ebelegi and D. Wankasi: *J. Chem*. 2017. https://doi.org/10.1155/2017/3039817.
30. L. Bartoňová, L. Ruppenthalová, and M. Ritz: *Chin. J. Chem. Eng*., 2017, vol. 25, pp. 37–44.
31. R. Saadi, Z. Saadi, R. Fazaeli, and N.E. Fard: *Korean J. Chem. Eng*., 2015, vol. 32, pp. 787–99.
32. P.K. Ackerman, G.H. Harris, R.R. Klimpel, and F.F. Aplan: *Int. J. Miner. Process*., 1987, vol. 21, pp. 105–27.